

Fig. 1. Phases encountered in this study. The diagram is a projection, in mole percent, from the H_2O apex onto the $\text{MgO}-\text{Al}_2\text{O}_3-\text{SiO}_2$ plane.

Chernosky (1974) redetermined the position of reaction (1) with reversed experiments, using synthetic crystalline phases as starting materials (Fig. 2). He also examined the variation in chlorite composition by measuring d_{004} and found no evidence for compositional variability at water pressure up to 2 kbar. His work provides the best estimate for the reaction coordinates at lower pressures.

In their high pressure experiments (up to 35 kbar), Staudigel and Schreyer (1977) also reported no shift in clinocllore composition. However, Jenkins (1980, 1981) indicated that chlorite becomes more aluminous than the clinocllore composition with increasing temperature at pressures above 4 kbar, and that the compositional shift in chlorite composition may be dominantly temperature-dependent.

Two major aspects of clinocllore synthesis with which this study is concerned are the conversion of the 7 Å to 14 Å structure and the possibility of compositional variation in clinocllore, which appear to be kinetically controlled processes. To investigate these kinetic problems in clinocllore synthesis, long runs up to 249 days were conducted at 2 kbar water pressure, using oxide mixtures of clinocllore composition as starting material.

Preliminary results reporting aspects of this work were given by Cho and Fawcett (1982).

Experimental methods

All runs were conducted at 2 kbar (29000 p.s.i.) water pressure using conventional hydrothermal techniques. Details are described by McOnie et al. (1975) and Cho (1982). Temperatures of the experiments were monitored by internally fitted chromel-alumel thermocouples ($\frac{1}{16}$ inch O.D.), and measured by either a KAYE 8000 multichannel recorder or a Leeds and Northrup potentiometer (model 8690-2) using zero degrees centigrade as a reference temperature. Each internal thermocouple and the

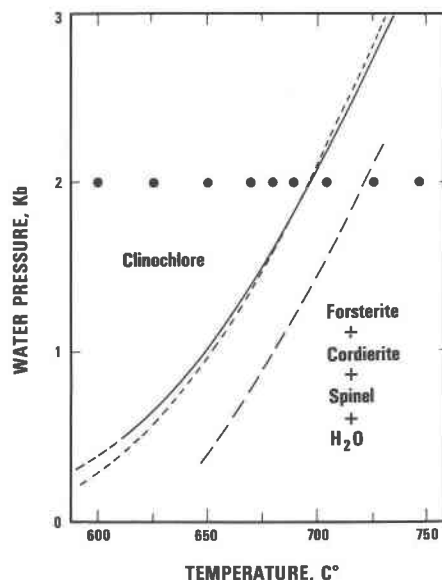


Fig. 2. Dissociation curves for the reaction clinocllore = forsterite + cordierite + spinel + vapour. Solid curve is for the reaction involving anhydrous cordierite and short-dashed one for the reaction involving 1.8 wt.% H_2O in cordierite (Chernosky, 1974). Dashed line is the dissociation curve determined by Yoder (1952). The dots indicate the experimental conditions employed in this study.

associated measuring and recording circuitry were calibrated against the melting point of NaCl (800.4°C). Uncertainties in run temperatures are a combination of the thermal gradient over the capsule length ($\pm 2^\circ\text{C}$, Cermignani, 1979), uncertainty in thermocouple calibration ($\pm 2^\circ\text{C}$) and the variance of the day-to-day fluctuations in recorded temperature (± 0.5 to $\pm 3^\circ\text{C}$; 1 standard deviation), and total ± 4.5 to $\pm 7^\circ\text{C}$. Pressures were measured on a 50000 p.s.i., 11-inch-diameter Heise gauge (manufacturer's certified accuracy ± 50 p.s.i. at all pressures) and are believed to be accurate to ± 100 p.s.i.

The starting material was an oxide mix of MgO , Al_2O_3 and SiO_2 in the stoichiometric proportion of clinocllore composition ($5\text{MgO} \cdot \text{Al}_2\text{O}_3 \cdot 3\text{SiO}_2$). The following reagents were used in preparation of the oxide mixture: Magnesium carbonate-Fisher Certified Reagent (lot 762372) heated in air to produce MgO ; aluminum hydroxide-Fisher Certified Reagent (lot 791077) heated in air to produce λ -alumina; silica glass-Specpure JMC 425 fired overnight at 900°C to drive off absorbed water. SEM observation revealed that the grain size of the oxide mix was less than 15 μm and averaged about 3 μm .

Starting materials were weighed into the annealed gold tubes (2.5 cm in length) with excess water, which was approximately equal to 25 wt.% of the charge. In most cases one capsule was run per experiment. By pre-heating the furnaces it was possible to reduce the warm-up time to about 30 minutes which served to minimize the kinetic effect of warm-up on the final run product. Reported "run duration" times do not include the warm-up time. Quench time (to room temperature) was less than 3 minutes.

The products of each experiment were examined with a binocular and petrographic microscope, and by X-ray powder diffractometry. Due to the extremely fine-grained nature of most of the run products, identification was based exclusively on X-ray diffraction (XRD) methods. A Philips X-ray diffractometer, em-

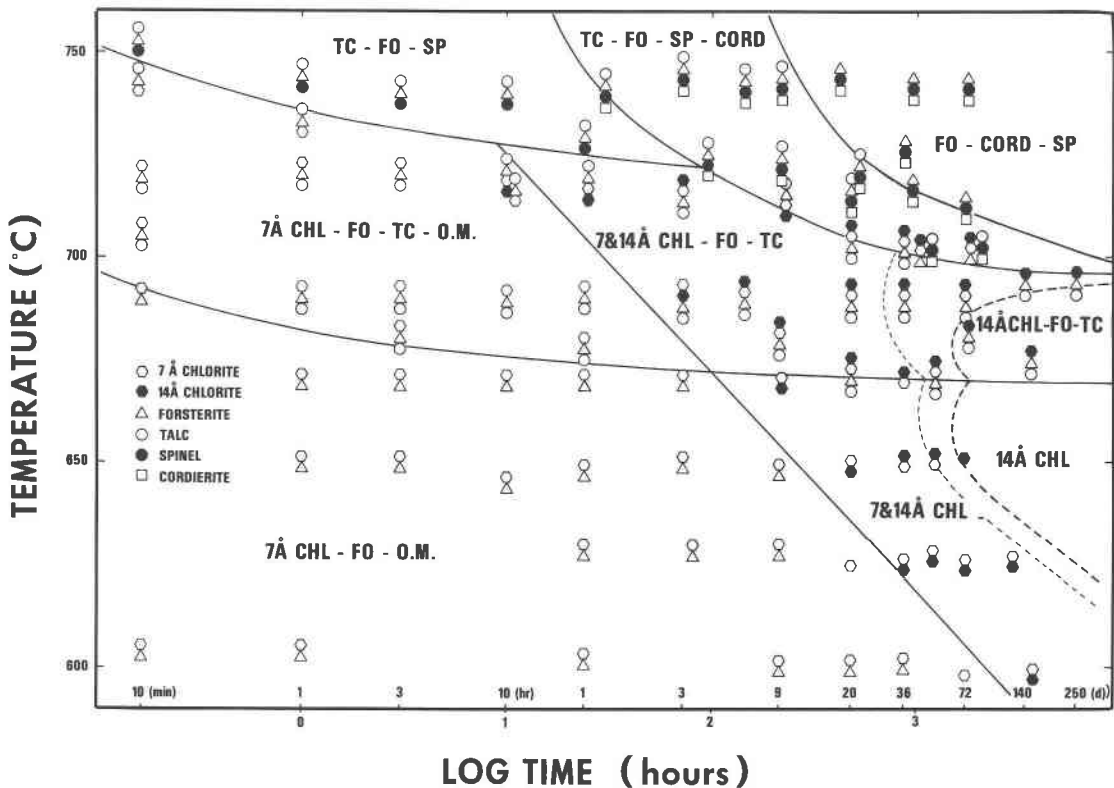


Fig. 3. A TTT diagram for the synthesis of clinocllore and forsterite + cordierite + spinel. Long-dashed curve is the calculated line for the complete conversion of 7 Å chlorite to 14 Å chlorite and short-dashed curve for 75% conversion. Some runs that merely confirm the boundaries as shown, are not plotted for clarity. Abbreviations: Chl (chlorite), Fo (forsterite), Tc (talc), Sp (spinel), Cord (cordierite) and O.M. (oxide mix).

ploying Ni-filtered, $\text{CuK}\alpha$ radiation, was used to examine smear mounts on glass slides.

Selected samples of low temperature (below 694°C) assemblages were examined by electron microprobe to determine the chemical composition of the run products. Fragments of run products were mounted with epoxy on a glass slide and analyzed on an ARL instrument with an energy-dispersive, solid state detector, using accelerating potential of 20 kV and a beam diameter of approximately 2 μm .

Results

Mineral phases and their compositions encountered in this study are plotted in Figure 1. Temperature and run duration were varied to determine their effects on the kinetics of synthesis. In order to investigate synthesis of the clinocllore composition far below and above the equilibrium temperature of reaction (1), the temperatures of individual experiments varied from 600 to 750°C in 10 and 25 degree increments, and the run duration from 10 minutes to 249 days. The results of the experiments are presented in Table 1.

The time-temperature-transformation diagram

A TTT diagram (Putnis and McConnell, 1980) displaying the time dependent transformations at different temperatures has been established from the results of the various hydrothermal experiments for reaction (1) (Fig. 3).

Most boundaries delineating individual fields of the assemblages are well constrained by the synthesis experiments and appear to be curvilinear. They show negative slopes except the one for the disappearance of 7 Å chlorite, which shows a C-type curve typical of many TTT diagrams (Putnis and McConnell, 1980). Some runs at a particular temperature and duration were duplicated and the assemblages were found to be reproducible. For example, three 20 day runs were made at 689°C (runs 7, 30 and 31, Table 1); Runs 30 and 31 represent the duplicates from the two capsules loaded together in a pressure vessel. All three run products contain the same mineral assemblage of 14 and 7 Å chlorite + talc + forsterite, although the modal abundances of individual phases are slightly variable (see Table 1 for further examples).

At temperatures higher than 720°C, talc + forsterite + spinel occurs as a metastable phase assemblage in short duration runs, crystallizing earlier than the stable assemblage, forsterite + cordierite + spinel. The proportion of metastable talc increases gradually with time in runs of short duration. However, it decreases rapidly and finally becomes zero as the more stable cordierite appears and becomes more abundant with increasing run duration.

Below 740°C, 7 Å chlorite-forsterite-talc or 7 Å chlorite-forsterite assemblages have been identified in shorter runs. The occurrence of non-aluminous phases with chlorite requires additional material that is more aluminous

Table 1. Run data

Run No.	Temperatures in Degrees C.	Duration	Crystalline Products	I_r	X_{chl}
89	597.3±7.0, n=66	72d	7Å Chl		
90	598.1±7.7, n=106	156d	7 & 14Å Chl		
124	624.5±5.1, n=16	20d	7Å Chl		
46	624.9±5.5, n=34	36d	7 & 14Å Chl	0.10	14
131	627.1±6.0, n=14	50d	7 & 14Å Chl	0.14	20
123	625.7±7.0, n=37	122d	7 & 14Å Chl	0.30	43
34	648.1±5.2, n=9	9d	7Å Chl-tr. Fo		
33	648.9±4.9, n=18	20d	7 & 14Å Chl	0.21	30
126	650.6±6.7, n=19	51d	14 & 7Å Chl	0.61	87
129	650.9±6.7, n=26	70d	14Å Chl	0.66	94
56	670.1±4.5, n=2	1d	7Å Chl-tr. Fo		
60	669.9±5.8, n=5	3d	7Å Chl-tr. Fo		
53	669.4±5.4, n=15	9d	7 & 14Å Chl	0.18	26
95	672.3±5.1, n=18	20d	14 & 7Å Chl-tr. Fo	0.50	71
39	670.9±6.4, n=32	36d	14 & 7Å Chl	0.43	61
106	670.7±5.8, n=56	52d	14 & 7Å Chl-tr. Fo	0.54	77
108	670.7±5.8, n=56	52d	14 & 7Å Chl-tr. Fo	0.62	89
62	674.0±6.2, n=87	150d	14Å Chl-tr. Fo	0.66	94
122	680	3h	7Å Chl-Fo-tr. Tc		
116	676.6±6.1, n=3	1d	7Å Chl-Tc-Fo		
112	680.1±6.4, n=14	9d	14 & 7Å Chl-Tc-Fo	0.38	54
96	682.4±5.4, n=20	20d	14 & 7Å Chl-tr. Fo	0.50	71
102	681.8±5.5, n=41	36d	14 & 7Å Chl-tr. Fo	0.57	81
110	681.1±5.3, n=51	52d	14 & 7Å Chl-tr. Fo	0.62	89
97	681.5±5.4, n=71	72d	14Å Chl-tr. Fo	0.66	94
79	689.3±5.0, n=10	10m	7Å Chl-Fo		
37	690	1h	7Å Chl-Fo-tr. Tc		
36	690	3h	7Å Chl-Fo-tr. Tc		
12	689.7±4.5, n=6	1d	7Å Chl-Tc-Fo		
11	689.4±4.7, n=18	3d	7 & 14Å chl-Tc-Fo	0.35	50

Table 1. (cont.)

Run No.	Temperatures in Degrees C.	Duration	Crystalline Products	I_r	X_{chl}
7	689.5±4.8, n=119	20d	14 & 7Å Chl-tr. Fo	0.45	64
30	689.1±4.5, n=20	20d	14 & 7Å Chl-Tc-Fo	0.51	73
31	689.1±4.5, n=20	20d	14 & 7Å Chl-Tc-Fo	0.47	67
32	690.1±4.8, n=29	28d	14 & 7Å Chl-tr. Fo	0.51	73
19	689.8±4.5, n=34	36d	14 & 7Å Chl-Tc-Fo	0.53	76
24	689.5±5.3, n=66	72d	14 & 7Å Chl-tr. Fo	0.60	86
27	689.5±5.3, n=66	72d	14 & 7Å Chl-tr. Fo	0.61	87
111	692.8±5.8, n=73	109d	14 & 7Å Chl-tr. Fo	0.65	93
29	693.5±6.6, n=84	140d	14Å Chl-tr. Tc-tr. Fo	0.70	100
28A	693.2±6.3, n=150	249d	14Å Chl-tr. Tc-tr. Fo	0.68	97
91	708.6±4.8, n=10	10m	7Å Chl-Fo-tr. Tc		
105	704.2±5.1, n=20	20d	14 & 7Å Chl-Tc-Fo	0.53	76
103	702.6±6.4, n=42	36d	14 & 7Å Chl-Tc-Fo	0.53	76
119	701.3±5.6, n=29	46d	14 & 7Å Chl-Tc-Fo-tr. Cord	0.59	84
104	702.1±6.2, n=71	82d	14 & 7Å Chl-Tc-Fo-tr. Cord	0.66	94
67	716.2±4.5, n=2	11h	Tc-Fo-7Å Chl		
80	717.5	1d	Tc-Fo-7 & 14Å Chl		
63	713.8±4.8, n=5	3d	14 & 7Å Chl-Tc-Fo		
70	717.1±4.5, n=8	9d	Tc-Fo-14 & 7Å Chl-Sp(?)		
55	715.8±4.9, n=12	20d	Tc-Fo-Sp-Cord		
57	716.9±5.2, n=16	40d	Fo-Cord-Sp		
73	712.1±6.2, n=53	72d	Cord-Fo-Sp		
98	719.6±5.4, n=3	10h	Tc-7 & 14Å Chl-Fo		
93	729.4±4.5, n=5	1d	Tc-Fo-Sp		
82	724.0±6.1, n=4	4d	Tc-Fo-Sp-Cord		
100	722.7±4.9, n=9	9d	Tc-Fo-Sp-Cord		
84	721.1±4.8, n=15	21.8d	Tc-Fo-Cord-Sp		
72	725.7±6.0, n=25	36d	Cord-Fo-Sp		
76	742.3±5.3, n=10	10m	Fo-Tc-7Å Chl		
92	752.5±5.8, n=10	10m	Tc-Fo-Sp		
77	743	1h	Tc-Fo-Sp		
118	740	10h	Tc-Fo-Sp		
68	741.1±6.4, n=2	1.5d	Tc-Fo-Sp-tr. Cord		
83	744.1±6.4, n=2	3d	Tc-Fo-Sp-tr. Cord		
65	742.7±7.1, n=8	9d	Tc-Fo-Sp-Cord		
52	740.3±5.2, n=18	17d	Fo-Sp-Cord		

Abbreviations: Chl (Chlorite), Fo (Forsterite), Tc (Talc), Sp (Spinel), Cord (Cordierite), m (minute), h (hour), d (day) and tr. (trace)

* I_r = Intensity ratio of (001) and (002) reflections of chlorite polymorphs.

** X_{chl} = Percent transformation of chlorite polymorphs.

The order of phases listed corresponds to one of decreasing intensity of their strongest characteristic peak, although the relative proportions of the phases identified could not be estimated reliably because of the preferred-orientation effect.

***n = number of temperature measurements.

than clinocllore composition. However, no phases other than chlorite, forsterite and talc appeared in XRD analyses. This may be attributed to a very small amount of the assumed aluminous phase(s), or to the amorphous nature of the assumed aluminous material. The latter may be the case since abundant isotropic aggregate, which appear to be partially-reacted oxide mixture, are detected by the petrographic microscope in shorter runs. The amorphous oxide mixture occurs as aggregates, composed of extremely fine grains of less than 0.5 μm size and the very fine grain size of this material precludes exact identification.

The occurrence of phases with little or no alumina, i.e., forsterite and talc, in addition to 7 Å chlorite may imply that the nucleation rates of forsterite and talc are greater than that of chlorite as pointed out by Staudigel and Schreyer (1977).

7 Å chlorite persists metastably for a very long time (over 72 days at 600°C) and finally converts to 14 Å chlorite through the mixture of 7 Å and 14 Å chlorite. The transformation of 7 Å chlorite to 14 Å chlorite will be discussed in detail in a later section.

In summary, the present experiments suggest that the assemblages chlorite-forsterite, below 670°C (Chernosky,

1975) and talc-forsterite-spinel (Yoder, 1952; Segnit, 1963) described by previous investigators, are metastable and crystallize earlier than the final stable assemblage but persist for long periods of time. Most stable phase assemblages are synthesized only through an intermediate assemblage, providing a good demonstration of Ostwald's rule of the prior formation of unstable phases. The gradual transformation of several metastable phase assemblages to final stable assemblages can be traced on the time-temperature-transformation diagram. The recognition of metastable phase assemblages using a TTT diagram shows that reactions are extremely sluggish both at low temperatures and near the reaction temperature. This provides further reinforcement of the need to demonstrate reaction reversals in phase equilibrium studies. Therefore, the importance of this diagram cannot be overemphasized in understanding solid state reactions. Unfortunately, at the present time very few TTT diagrams are available for metamorphic reactions.

Rate studies

Rate studies have been carried out for the transformation of 7 Å chlorite to 14 Å chlorite below the equilibrium temperature of reaction (1), using products of runs

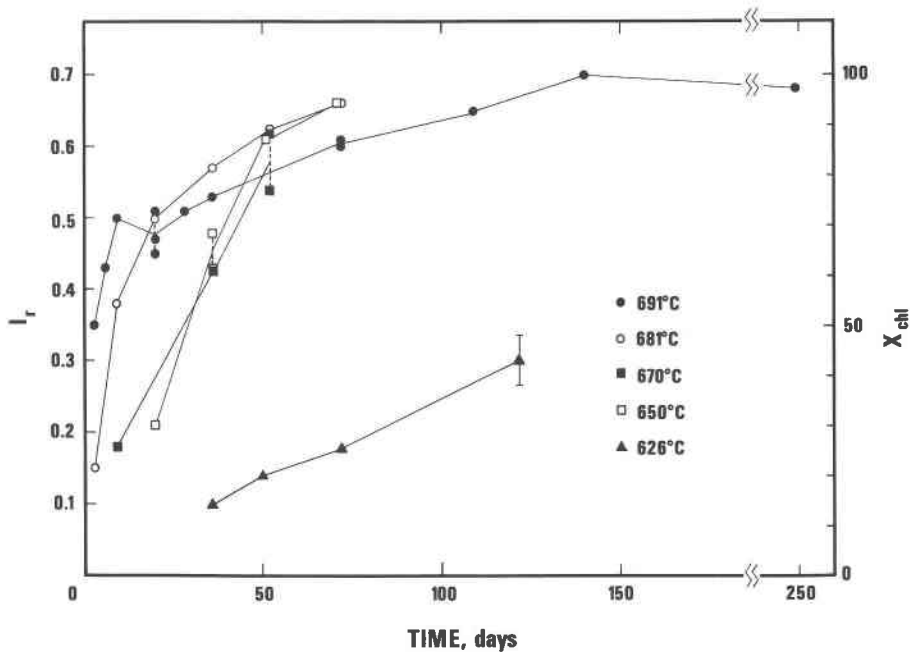


Fig. 4. Variation of I_r and X_{chl} as a function of run duration (in days). Mean experimental temperatures are 626, 650, 670, 681, and 691°C. Length of solid bar represents precision of measurement and dotted lines connect duplicate runs.

that yielded 7 Å and 14 Å chlorite assemblages. Quantitative determination of the extent of transformation was determined by measuring the peak heights from basal reflections of chlorite on powder X-ray diffraction charts. The relative intensities (I_r) of (001) and (002) basal reflections from a 7 Å and 14 Å chlorite mixture were used for quantitative analyses of 14 Å chlorite, because both 7 Å and 14 Å chlorites will orient to the same degree to eliminate the effect of the preferred orientation (Mossman et al., 1967). All samples were scanned three to eight times at 1°/minute to determine the ratios of the peak heights (Table 1). In calculating the percent reaction (X_{chl}), it is assumed that the intensity ratio of (001)/(002) for pure 14 Å chlorite is 0.7 which is the maximum value obtained in this study as shown in Figure 4. The ratio increases with run duration and reaches a steady state value of 0.7 in experiments of about 150 days. The precision of the method was estimated to be better than $\pm 10\% X_{chl}$.

Figure 4 is the plot of I_r versus run duration. Mean experimental temperatures were 626, 650, 670, 681, and 691°C. Duplicate runs are also plotted, which show a fluctuation of up to 15% X_{chl} . As a small degree of reaction cannot be determined by XRD, the initial stage of transformation at each specific temperature is difficult to define. Large uncertainties in X_{chl} also make it difficult to distinguish experimentally between the various solid state reaction models (Sharp et al., 1966). However, the curves connecting experimental data points appear to be parabolic in shape, with rapid initial reaction.

The simple model equation to best fit the experimental

data is the parabolic rate equation (Kridelbaugh, 1973; Matthews, 1980):

$$X_{chl} = k \cdot t^n \quad (2)$$

where X_{chl} is the percent of transformation, k , the rate constant, t is time in days, and n is the order of reaction. Writing equation (2) in logarithmic form:

$$\log X_{chl} = \log k + n \log t \quad (3)$$

gives a straight line with a slope of n and an intercept of $\log k$ in a $\log X_{chl}$ versus $\log t$ plot.

Figure 5 is the plot of experimental data at each temperature showing linear-regression lines based on equation (3). The values of the constants n and $\log k$ for equation (3) are presented in Table 2. Times for the 75% and complete conversion of 7 Å chlorite to 14 Å chlorite are calculated from the linear-regression equations at each temperature. They are also listed in Table 2 and plotted in Figure 3. As can be expected, it required very long durations for the complete conversion both at low temperature (312 days at 626°C) and near the reaction temperature. The apparent inflections at 670°C (Fig. 3) might indicate a change in reaction mechanism that will be discussed later.

The uncertainties in the above values are calculated by weighting the standard deviations at each data point (Bevington, 1969, Chapter 6). When the standard deviations (σ_1 and σ_2) for each data point are different because of the non-linear scale, the averages, $\sigma = (\sigma_1 + \sigma_2)/2$, are

taken throughout the study. Two different standard deviations for a few cases are listed together.

The order of reaction decreases gradually with increasing temperature from approximately 0.9 at 626 and 650°C to 0.15 at 691°C (Table 2). This variation in n indicates a change in the mechanism of the reaction (Busenberg and Plummer, 1982).

The rate constant (k) is related to an activation energy (H_a) by the Arrhenius equation:

$$k = A \exp(-H_a/RT) \quad (4)$$

where A is a temperature-independent frequency factor, R is the gas constant and T is the absolute temperature. Writing equation (4) in logarithmic form:

$$\log k = \log A - H_a/2.303RT \quad (5)$$

Therefore, the Arrhenius plot of $\log k$ versus $1/T$ gives a straight line of slope $-H_a/2.303RT$ and intercept $\log A$.

Figure 6 is the Arrhenius plot of k derived from equation (5). There is an apparent break in the slope at about 670°C, which indicates a change in reaction mechanism. An activation energy of 90 ± 35 kcal/mole (H_{a1}) was calculated at temperatures below 670°C and an activation energy of $177 \pm_{49}^{113}$ kcal/mole (H_{a2}) at temperatures between 670 and 691°C. The uncertainties in H_{a1} and H_{a2} are calculated by considering only the uncertainties in k and temperature, respectively. A single line, with no change in slope could be fitted to all five data points on Figure 6. We prefer the interpretation shown in the figure because independent evidence, discussed later in the paper, suggests a change in chlorite composition at about 670°C. Our interpretation of these data is also consistent with the inflection noted at this temperature for the boundary curves shown on Figure 3.

The high value of H_{a2} , as compared to H_{a1} can be related to the stable existence of forsterite + talc with 14 Å chlorite at about 670–696°C, as will be demonstrated in a later section. As the 14 Å chlorite in the chlorite-forsterite-talc assemblage is more aluminous than the ideal clinocllore composition, H_{a2} may represent the activation energy for the transformation of Mg-chlorite polymorphs that are more aluminous than the ideal clinocllore composition.

An activation energy larger than 90 kcal/mole might indicate that diffusion is probably not the rate-controlling step for the transformation of chlorite polymorphs (see Table 3). As suggested by Roy and Roy (1955), a number of Si–O bonds must actually be broken and rearranged, so that every alternate layer of Si^{4+} ions in the silica layer of 7 Å chlorite can form new Si–O bonds with the linked tetrahedra pointing in the opposite direction. Such a rearrangement of the Si–O bonds might be the rate-determining process for the transformation from 7 Å to 14 Å structure.

² Two different standard deviations due to the non-linear scale are listed together.

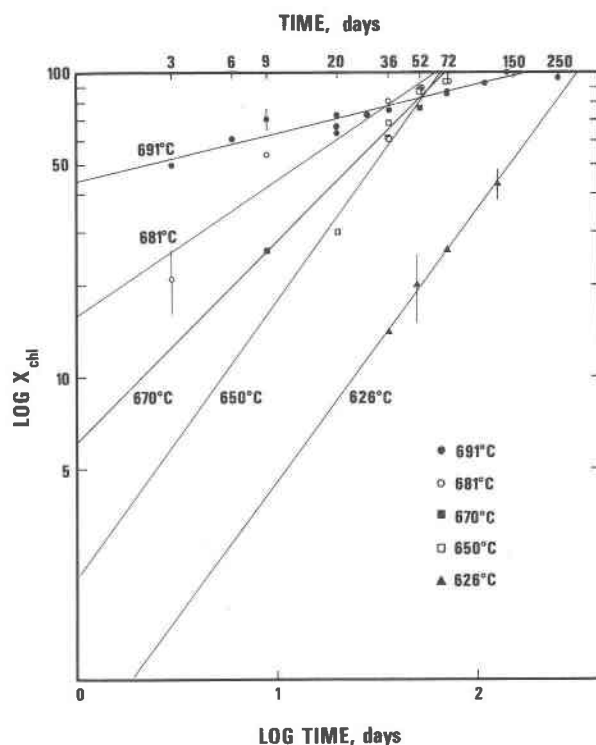


Fig. 5. A plot of $\log X_{\text{chl}}$ versus \log time (in days) showing linear-regression lines at each temperature. Symbols are the same as in Figure 4. Uncertainties on X_{chl} are all the same but appear different due to the log scale.

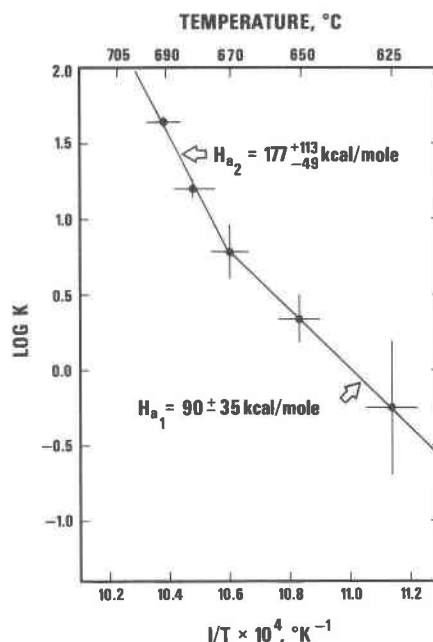


Fig. 6. The Arrhenius plot of $\log k$ versus $1/T$ (in degrees Kelvin). A change in the reaction mechanism is suggested by the change in slope at approximately 670°C.

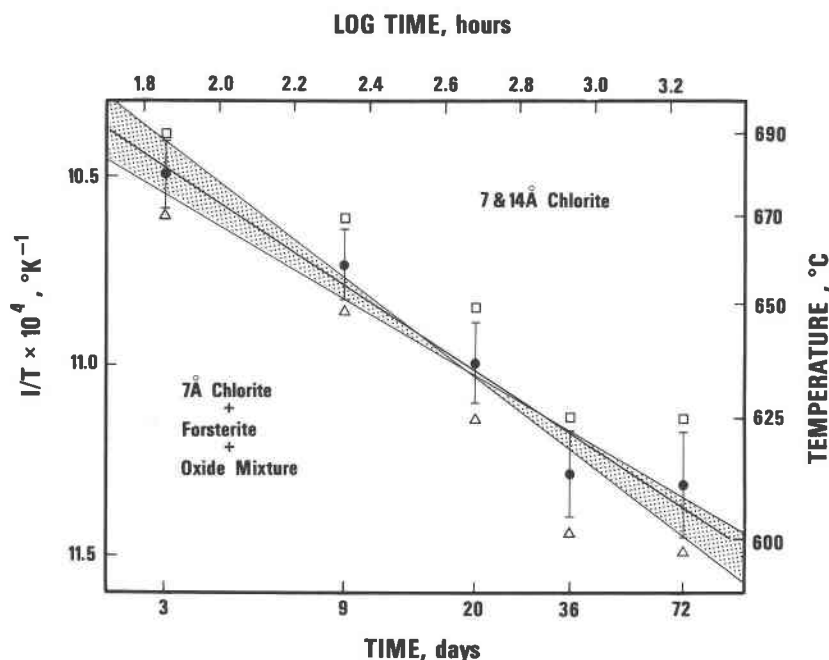


Fig. 7. A plot of log time against $1/T$ (in degrees Kelvin) showing the bracketing data (solid dots) between 7 Å chlorite-forsterite-oxide mixture (open triangle) and 7 Å and 14 Å chlorite (open rectangle). Thick solid line represents an estimate of the phase boundary between the two assemblages. Dotted area represents "envelope of uncertainty." *Three day runs are included in order to reduce the range of uncertainty. This does not affect the present interpretation because H_a without 3 day runs is 62 kcal/mole.

Nucleation activation energy of 14 Å chlorite

The activation energy for the nucleation of 14 Å chlorite from 7 Å chlorite-forsterite-oxide mixture can be calculated from the TTT diagram.

The rate of nucleation K at any temperature is the product of the thermodynamic factor and kinetic factor (Putnis and McConnell, 1980):

$$K = C \exp(-\Delta G^*/RT) \exp(-H_a/RT) \quad (6)$$

where C is constant, ΔG^* is free energy of activation for the formation of a critical nucleus, and H_a is activation energy for a kinetic process. Writing (6) in logarithmic form:

$$\ln K = \ln C - (\Delta G^*/RT) - (H_a/RT) \quad (7)$$

From equation (3), $\ln X_{chl} = \ln K + n \ln t$. Therefore,

$$n \ln t = (\Delta G^*/RT) + (H_a/RT) - \ln C' \quad (8)$$

where C' is constant. For all low temperatures $\Delta G^* \approx 0$ (Putnis and McConnell, 1980; Putnis and Bish, 1983), and

$$\ln t = H_a/nRT - \ln C'' \quad (9)$$

where C'' is constant. The activation energy for the nucleation of 14 Å chlorite can be found from the slope in the $\ln t$ versus $1/T$ plot at low temperatures. It should be noted that the activation energy for nucleation, calculated using the equation (9) represents the maximum value because ΔG^* is assumed to be zero.

The curve for the appearance of 14 Å chlorite is almost linear at temperatures below 670°C (Fig. 3). Experimental data are plotted again in Figure 7 on a log t versus $1/T$ diagram to define the curve for the first appearance of 14 Å chlorite. The uncertainties in the bracketing data between the two assemblages were calculated using equation 6a of Demarest and Haselton (1981). Only the uncertainties in temperature are considered since the errors in run duration plotted in log scale are small in long runs. An activation energy of 63^{+8}_{-8} kcal/mole was calculated for the first appearance of 14 Å chlorite from the TTT curve, using $n = 0.9$ (from Table 2), as compared to a value of 90 ± 35 kcal/mole from the rate study. The errors are taken from the slopes of two extreme lines.

The activation energy calculated from the TTT curve is smaller than the activation energy obtained from the rate studies, implying that nucleation is not the rate-controlling mechanism. However, because of large uncer-

Table 2. Values of the constants n and $\log k$ for the equation, $\log X_{chl} = \log k + n \log t$, and the calculated times for the 75% and complete conversion of 7 Å chlorite to 14 Å chlorite at each experimental temperature

Temperature (°C)	n	$\log k$	Time for conversion (days)	
			75%	100%
625.6	0.902±0.227	-0.2504±0.4464	226.7±58.8	311.8±112.9
650.2	0.918±0.096	0.3385±0.1624	47.1±0.2	64.5±1.9
670.4	0.655±0.107	0.7854±0.1782	46.0±0.6	71.3±6.3
681.4	0.449±0.041	1.2015±0.0648	31.7±0.5	60.2±2.5
690.5	0.158±0.016	1.6444±0.0287	29.0±2.3	179.2±19.4

Table 3. Activation energy scale (kcal/mole); from Fyfe et al. (1978)

3-9	Dehydration and hydration
12-20	Migration of alkali cations through open structures
15-30	Exchange diffusion of Na, K, interstitial (vacancy) diffusion
25-40	Displacive transformation
50-70	Exchange migration of Si, Al
60-90	O-Si-O bonds from non-bridging oxygens
100-200	Lattice energies, break up of O-Si-O bonds

tainties involved, there is still a possibility that nucleation of 14 Å chlorite is a rate-controlling process. In this case, the difference in calculated activation energies could be attributed to two factors. First, small amounts of forsterite and oxide mixture coexisting with 7 Å chlorite might have decreased the activation energy for the conversion of 7 Å chlorite to 14 Å chlorite by providing appropriate material for nucleation of 14 Å chlorite. Second, the activation energy obtained from the TTT curve may represent an activation energy of a heterogeneous transformation, since the charge container may have provided heterogeneous nucleation sites and decreased the activation energy for the appearance of 14 Å chlorite. Heterogeneous phenomena in nucleation and growth of chlorites are ubiquitous in the run products, as demonstrated in the SEM study (Cho and Fawcett, 1986).

Chlorite-forsterite-talc assemblage

This assemblage was first identified by Fawcett and Yoder (1966) in 3.5 kbar water pressure experiments and was interpreted by them to be a stable one in which Mg-chlorite becomes more aluminous than clinochlore composition. Jenkins (1980, 1981) further indicated this shift in composition at pressures above 4 kbar. At 14 kbar and 850°C he estimated the composition of the most stable chlorite to be $(Mg_{4.88}Al_{1.12})(Si_{2.88}Al_{1.12})O_{10}(OH)_8$. Chernosky (1974) did not detect any compositional variability for water pressures up to 2 kbar and concluded that the most stable Mg-chlorite is of clinochlore composition.

Several longer runs, up to 249 days, were conducted at temperatures between 670° and 693°C, in order to investigate the stability or metastability of the chlorite-forsterite-talc assemblage. This assemblage persisted in each of those runs, even beyond the time calculated for the complete conversion of 7 Å chlorite to 14 Å chlorite (Fig. 3). The 150 day experiment at 674°C helps confirm the persistence of the assemblage and, together with shorter duration runs, establishes temperature limits for the chlorite-forsterite-talc assemblage (Fig. 3). Field boundary configurations on the TTT diagram strongly suggest that this assemblage is stable over a relatively narrow temperature interval.

To investigate the stability of the chlorite-forsterite-

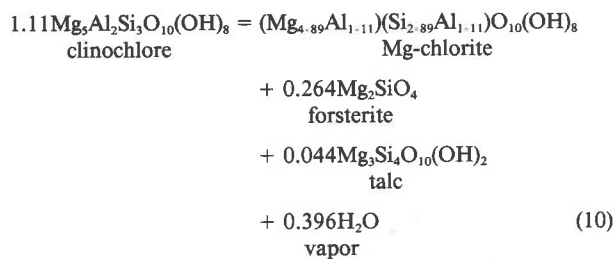
Table 4. Representative electron microprobe analyses of two selected chlorites

Sample No.	39	24
Temperature (°C)	670.9	689.5
Duration (days)	36	72
<u>Oxides wt. %</u>		
MgO	31.74	29.81
Al ₂ O ₃	17.22	16.90
SiO ₂	28.17	26.47
Total	77.13	73.19
<u>Ions (based on 14 oxygen atoms)</u>		
Mg	4.939	4.889
Al	2.120	2.192
Si	2.941	2.912

talc assemblage, the peak position of the d_{004} reflection was determined for 14 Å chlorite obtained in runs longer than 3 days (Chernosky, 1974). Three to eight oscillations were made from 24.5 to 27° 2θ at a scanning speed of 1/4° 2θ/min., using quartz as an internal standard. The serpentine determinative curve (Chernosky, 1975) which is also applicable for 14 Å chlorite (Schiffman and Liou, 1980) was used to estimate the Al content of these synthetic chlorites. The precision of this method is $\pm 0.015^\circ 2\theta$ (CuKα), which corresponds to a compositional variation of about $x = \pm 0.04$ in the formula, $(Mg_{6-x}Al_x)(Si_{4-x}Al_x)O_{10}(OH)_8$ (Caruso and Chernosky, 1979).

Several electron microprobe analyses of chlorite were performed to calibrate the XRD measurement of chlorite composition. Unfortunately, the analyses always gave lower totals than the ideal chlorite composition by 10–15%, which may be accounted for by the porous nature of the disaggregated chlorites (Table 4). However, a few analyses showing good chlorite stoichiometry proved to be consistent with XRD results, especially in the 690°C run product.

The results are listed in Table 5 and illustrated in Figure 8. It is evident that with increasing temperature there is a sudden decrease in d_{004} spacing at about 670°C, and that the chlorite composition varies from pure clinochlore at temperatures below 670°C to more aluminous chlorite of the approximate composition with $x = 1.11 \pm 0.04$ at temperatures between 680 and 693°C. This x value is consistent with $x = 1.12$ obtained at 14 kbar by Jenkins (1981). Therefore, the maximum stability of clinochlore is defined not by reaction (1) but by an overall reaction such as:



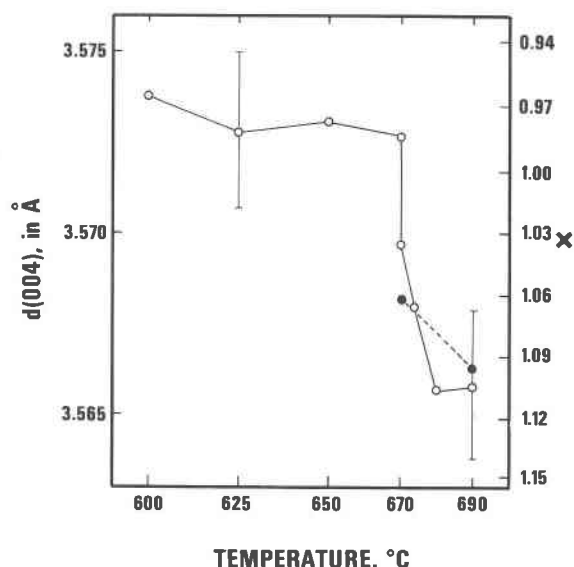


Fig. 8. Variation of d_{004} and Al content in terms of x value in synthetic chlorites as a function of temperature. Open circles represent the analyses determined by XRD and solid dots by electron microprobe.

whose reaction temperature is approximately 670°C at 2 kbar water pressure. Further detailed studies are required in order to characterize the reaction governing the transformation of clinocllore to the more aluminous chlorite, because Figure 8 does not preclude the possibility of a continuous reaction involving the coupled substitution of $2\text{Al} = \text{Mg} + \text{Si}$ in chlorite. If the latter is true, clinocllore will gradually change its composition towards the more aluminous chlorite ($x = 1.11$) within a short temperature interval of less than 20°C at 2 kbar water pressure.

The upper thermal stability of the most stable Mg-chlo-

Table 5. Variation in d_{004} of chlorite and the calculated x values, using the calibration curve of Chernosky (1975)

Run no.	Duration Temperature		x values		
	in days	(°C)	2θ (004)	d(004)	XRD microprobe
90	156	598.1	24.914	3.574	0.965
131	50	627.1	24.923	3.573	0.986
125	72	624.7	24.921	3.573	0.981
123	122	625.7	24.917	3.573	0.972
34	9	648.1	24.926	3.572	0.993
33	20	648.9	24.919	3.573	0.976
43	36	650.4	24.928	3.572	0.998
126	51	650.6	24.910	3.574	0.955
129	71	650.9	24.920	3.573	0.979
60	3	669.9	24.944	3.570	1.036
53	9	669.4	24.922	3.573	0.983
39	36	670.9	24.943	3.570	1.034
62	150	674.0	24.953	3.568	1.065
102	36	681.8	24.974	3.565	1.112
97	72	681.5	24.970	3.566	1.102
11	3	689.4	24.872	3.566	1.107
7	20	689.5	24.967	3.566	1.094
32	28	690.1	24.958	3.658	1.071
24	72	689.5	24.969	3.566	1.099
27	72	689.5	24.971	3.566	1.104
29	140	693.5	24.976	3.565	1.117
29A	249	693.2	24.972	3.566	1.107

rite with $x = 1.11$ can be estimated from the TTT diagram. In runs longer than 46 days at 701°C, cordierite and spinel have formed together with the chlorite-forsterite-talc assemblage, suggesting that the latter assemblage is not the stable one above 701°C. This is also consistent with Chernosky's (1974) bracketed reaction temperature of $696 \pm 10^\circ\text{C}$. Yoder's (1952) reaction temperature which is 20 degrees higher than that of this study probably resulted from the metastable persistence of the chlorite-forsterite-talc assemblage above the equilibrium reaction temperature. Thus the importance of reversals in classical synthesis experiments cannot be overemphasized in determining phase equilibria.

Acknowledgments

This study represents part of M. Cho's M.Sc. thesis at the University of Toronto. Dr. J. M. Allen and Dr. G. M. Anderson have contributed greatly in discussions during the course of this work. The research was supported by grants from the Natural Sciences and Engineering Research Council of Canada to J. J. Fawcett and by the H. V. Ellsworth Fellowship in Mineralogy at the University of Toronto (M. Cho). Reviews of a preliminary version of this manuscript by J. M. Allen, J. V. Chernosky, D. A. Hewitt, D. M. Jenkins, J. G. Liou and T. P. Loomis resulted in significant improvements to the presentation.

References

- Bevington, P. R. (1969) Data Reduction and Error Analysis for the Physical Sciences. McGraw-Hill Inc., New York.
- Busenberg, E. and Plummer, L. N. (1982) The kinetics of dissolution of dolomite in $\text{CO}_2\text{-H}_2\text{O}$ systems at 1.5 to 65°C and 0 to 1 atm P_{CO_2} . American Journal of Science, 282, 45-78.
- Caruso, L. J. and Chernosky, J. V., Jr. (1979) The stability of lizardite. Canadian Mineralogist, 17, 757-769.
- Cermignani, C. (1979) Metamorphic reactions in the system albite-anorthite-nepheline- $\text{Na}_2\text{CO}_3\text{-CaCO}_3\text{-H}_2\text{O}$, with application to the Haliburton-Bancroft alkaline rocks. Unpublished Ph.D. thesis, Univ. of Toronto.
- Chernosky, J. V., Jr. (1974) The upper stability of clinocllore at low pressure and the free energy of formation of Mg-cordierite. American Mineralogist, 59, 496-507.
- Chernosky, J. V., Jr. (1975) Aggregate refractive indices and unit cell parameters of synthetic serpentine in the system $\text{MgO-Al}_2\text{O}_3\text{-SiO}_2\text{-H}_2\text{O}$. American Mineralogist, 60, 200-208.
- Cho, M. (1982) A kinetic study of the clinocllore composition at 2 kbar water pressure. Unpublished M.Sc. thesis, Univ. of Toronto.
- Cho, M. and Fawcett, J. J. (1982) Mechanisms and kinetics of the reaction clinocllore = forsterite + cordierite + spinel + vapour. (abstr.). Transactions of the American Geophysical Union (EOS), 63, 465.
- Cho, M. and Fawcett, J. J. (1986) Morphologies and growth mechanisms of synthetic Mg-chlorite and cordierite. American Mineralogist, 71, 78-84.
- Demarest, H. H., Jr. and Haselton, H. T., Jr. (1981) Error analysis for bracketed phase equilibrium data. Geochimica et Cosmochimica Acta, 45, 217-224.
- Fawcett, J. J. and Yoder, H. S., Jr. (1966) Phase relationships of chlorites in the system $\text{MgO-Al}_2\text{O}_3\text{-SiO}_2\text{-H}_2\text{O}$. American Mineralogist, 51, 353-380.
- Fyfe, W. S., Price, N. J., and Thompson, A. B. (1978) Developments in Geochemistry, Vol. 1: Fluids in the Earth's Crust. Elsevier Scientific Publishing Company, Amsterdam.
- Greenwood, H. J. (1963) The synthesis and stability of anthophyllite. Journal of Petrology, 4, 317-351.

- Jenkins, D. M. (1980) Crystallochemical characterization of synthetic Mg-chlorite. (abstr.) Geological Society of America Abstracts with Programs, 12, 455.
- Jenkins, D. M. (1981) Experimental phase relations of hydrous peridotites modelled in the system H_2O -CaO-MgO- Al_2O_3 - SiO_2 . Contributions to Mineralogy and Petrology, 77, 166-176.
- Kridelbaugh, S. J. (1973) The kinetics of the reaction: calcite = quartz + wollastonite + carbon dioxide at elevated temperatures and pressures. American Journal of Science 273, 757-777.
- Lasaga, A. C. and Kirkpatrick, R. J. (1981) Kinetics of Geochemical Processes. Reviews in Mineralogy, vol. 8. Mineralogical Society of America, Washington, D.C.
- Matthews, A. (1980) Influences of kinetics and mechanism in metamorphism: a study of albite crystallization. Geochimica et Cosmochimica Acta, 44, 387-402.
- McOnie, A. W., Fawcett, J. J., and James, R. S. (1975) The stability of intermediate chlorites of the clinochlore-daphnite series at 2 kbar P_{H_2O} . American Mineralogist, 60, 1047-1062.
- Mossman, M. H., Freas, D. H., and Bailey, S. W. (1967) Orienting internal standard method for clay mineral X-ray analyses. Clays and Clay Minerals, 15, 441-453.
- Nelson, B. W. and Roy, R. (1958) Synthesis of the chlorites and their structural and chemical constitutions. American Mineralogist, 43, 707-725.
- Putnis, A. and McConnell, J. D. C. (1980) Principles of Mineral Behaviour. Elsevier, New York.
- Putnis, A. and Bish, D. L. (1983) The mechanism and kinetics of Al,Si ordering in Mg-cordierite. American Mineralogist, 68, 60-65.
- Roy, D. M. and Roy, R. (1955) Synthesis and stability of minerals in the system MgO- Al_2O_3 - SiO_2 - H_2O . American Mineralogist, 40, 147-178.
- Schiffman, P. and Liou, J. G. (1980) Synthesis and stability relations of Mg-Al pumpellyite, $Ca_4Al_3MgSi_6O_{21}(OH)_7$. Journal of Petrology, 21, 441-474.
- Segnit, R. E. (1963) Synthesis of clinochlore at high pressures. American Mineralogist, 48, 1080-1089.
- Sharp, J. H., Brindley, G. W., and Achar, B. N. N. (1966) Numerical data for some commonly used solid state reaction equations. American Ceramic Society Journal, 49, 379-382.
- Staudigel, H. and Schreyer, W. (1977) The upper thermal stability of clinochlore $Mg_3Al(AlSi_3O_{10})(OH)_8$, at 10-35 kb P_{H_2O} . Contributions to Mineralogy and Petrology, 61, 187-198.
- Yoder, H. S., Jr. (1952) The MgO- Al_2O_3 - SiO_2 - H_2O system and the related metamorphic facies. American Journal of Science, Bowen vol., 569-627.

*Manuscript received, December 1, 1983;
accepted for publication, September 9, 1985.*